48th AIAA Aerospace Sciences Meeting Including the New Horizons Forum and Aerospace Exposition
4 - 7 January 2010, Orlando, Florida

AIAA 2010-99

Turbulent Particulate Pressure for Two-Phase Flow Modeling

Claude HUG* and Pierre BRENNER†
EADS Astrium Space Transportation, 78 133 Les Mureaux, France

and

François DUBOIS‡
Conservatoire National des Arts et Métiers, Paris, France

[Abstract]: The simulation of two-phase turbulent flows is currently an important scientific and industrial challenge. Among the many issues underlying the modeling of that complex phenomenology, the accumulation of solid particles in preferential zones and the interaction of particles with gas turbulence are of particular interest, because they have a significant impact on the overall performance of the studied system.The objective of this work is to propose an original numerical model to solve problems of particulate concentration occurring in laminar or turbulent convergent two-phase flows. The formulation, expressed in the Eulerian framework, uses a particulate pressure and a pseudo particulate viscosity. Firstly the new hyperbolic system for pure particulate gas is analyzed in terms of consistency and numerical robustness. Existence of entropy and appropriate numerical schemes for the Riemann problem are discussed and tested in a one dimensional shock tube application. Secondly the whole system with the pseudo viscous terms and the source terms is explained. The coupling with the gas flow is especially derived in laminar or turbulent case. In particular the development of a space marching Parabolized Navier Stokes code for 2D axi-symmetric flow is presented. Implementation of the method in a fully 3D time dependent Navier Stokes code is under work. First encouraging applications of the axi-symmetric PNS code are presented. Comparisons with a classical two-phase flow formulation, without particulate pressure are performed. It indicates how efficient the new model is regarding the undesired axial accumulation of heavy particles. Also different Riemann solvers are tested.

Nomenclature

c, c_r, c_ℓ	=	pseudo sound speed
d	=	particle diameter
DNS	=	Direct Numerical Simulation
E	=	total energy
H	=	enthalpy
k, k_p, k_f	=	fluctuating kinetic energy
M	=	Mach number
NS	=	Navier Stokes
P, P_p	=	pressure

* R & D Engineer Thermal-Aerodynamics-Signatures Department: claude.hug@astrium.eads.net
† CFD Expert Thermal-Aerodynamics-Signatures Department: pierre.brenner@astrium.eads.net
‡ Professor of Applied Mathematics, duboisf@cnam.fr

P_{kp} = production term of k_p

PNS = Parabolized Navier Stokes

$u, v, w, U_{p,i}, U_{f,i}$ = mean velocity components

$u'_{p,i}, u'_{f,i}$ = fluctuating velocity components

T = temperature

T^* = integral time scale

γ = tensor parameter $\gamma = 5/3$

ι = internal particle energy

ρ, ρ_p, ρ_f = density

ν_p = pseudo cinematic viscosity

$< \tau_p >$ = mean particle relaxation time

Subscript:

$_p$ = particulate

$_f$ = fluid or gas

$_r$ = right

$_\ell$ = left

$_i$ or $_j$ = Cartesian coordinates

I. Problem position

The Eulerian formulation is very practical for engineer modelling of two-phase flows. The approach suits a wide range of particles in turbulent fluid and is currently recommended before using more time consuming modelling like lagrangian or DNS (see Ref. 1). The Eulerian framework allows the use of the same mesh for gas and particles, and is generally less expensive in computer time and memory. In aerospace applications, like two-phase rocket plume for instance, particles can be considered as a dispersed phase, where volume occupancy or collisions can be neglected. As a matter of fact, the particulate flow is modelled like a gas without pressure. This simplifies the equations, and namely for the Riemann problem, a simple "donor cell" scheme is sufficient.

One drawback, which may also appear in Lagrangian formulation, is that particle accumulation in preferential region can occur in the simulation. Because of the complexity of the phenomenology, engineers have to face a real problem: is this accumulation a numerical artefact related to the method? or is it a physical description? The answer is not obvious because concentrations occur for specific configurations in the physical world.

For a convergent axi-symmetric flow of a particulate gas without pressure (with the eulerian formulation), the axis is a singularity where particulate density in the mixture goes to infinity, as shown by Saurel[2].

The proposed solution is to introduce a particulate pressure, which was also done by Saurel & Abgrall[3], Simonin[4], Simoes & al[5,6,7], in different ways.

In the present work, this particulate pressure is only related to the fluctuating particle velocity and density in the mixture. In particular, there is no direct relation between that pressure and the particle internal energy ι, which exhibits fundamental differences with a gas pressure. The fluctuating velocity applies in laminar gas flow (it does then represent the Brownian motion), and in turbulent gas flow (it is then added the coupling with turbulent gas velocity fluctuations by the covariance). The model follows the engineering methods proposed in the book of Oesterlé[8], and is implemented in an existing two-phase turbulent and reactive PNS code.

II. Hyperbolic system of conservation laws

We introduce the density ρ of the gas of particles, the velocity u, internal energy ι and turbulent kinetic energy k Total energy is the sum of kinetic energy, internal energy and turbulent kinetic energy:

$$E = \frac{1}{2}u^2 + \iota + k. \quad (1)$$

The variables of specific mass ρ, momentum ρu, and total massic energy ρE are naturally conserved. Moreover, we suppose here that the volumic turbulent kinetic energy ρk is also conserved. We can introduce a vector W with four coordinates according to

(2) $$W = (\rho, \rho u, \rho E, \rho k)^t.$$

The associated vector flux $f(W)$ follows classical results of gas dynamics (see *e g* Landau and Lifchitz[9]). We have:

(3) $$f(W) = (\rho u, \rho u^2 + p, \rho u E + p u, \rho u k)^t.$$

Then the particle-gas system can be written in one space dimension as a conservative system of a four-dimensional vector $W(x,t)$

(4) $$\frac{\partial W}{\partial t} + \frac{\partial}{\partial t}(f(W)) = 0.$$

The system is mathematically entirely defined if the pressure can be evaluated from the conserved variables. Following Hug[10], we set

(5) $$p = (\gamma - 1)\rho k$$

with $\gamma > 1$ a constant that parameterizes the model. The pressure does **not** depend anymore on the internal energy as in an usual gas (see *e g* Ref. 9) and the physical hypothesis is constitutive of what we call here "particle-gas system".

The previous system is hyperbolic and exhibits four eigenvalues:

(6) $$\lambda_1 \equiv u - c < \lambda_2 = \lambda_3 \equiv u < \lambda_4 \equiv u + c$$

The sound velocity c is simply obtained by a non-standard relation

(7) $$c = \sqrt{\frac{p}{\rho}} = \sqrt{(\gamma - 1)k}$$

as proven in Ref. 11

The fields numbered with indexes 1 and 4 are genuinely nonlinear (*e g* the book of Godlewski and Raviart[12]). The second (identical to the third) field is linearly degenerated. The corresponding Riemann invariants β_j (that are constant in rarefaction waves and inside contact discontinuities) are given according to

(8) $$\begin{cases} \beta_1 \in \{k, u + c\log\rho, \iota - c^2\log\rho\} \\ \beta_2, \beta_3 \in \{u, p\} \\ \beta_4 \in \{k, u - c\log\rho, \iota - c^2\log\rho\} \end{cases}$$

A shock wave of velocity σ between a given state W_ℓ and an "aval" state W satisfies the following algebraic relations[11]:

(9) $$\begin{cases} \rho(u - \sigma) = \rho_\ell(u\ell - \sigma) = c_\ell\sqrt{\rho\rho_\ell} \\ k = k_\ell \\ u - u\ell = -\dfrac{c_\ell}{\sqrt{\rho\rho_\ell}}(\rho - \rho_\ell) \\ p = {c_\ell}^2(\rho - \rho_\ell) \\ \iota - \iota_\ell = \dfrac{{c_\ell}^2}{2\rho\rho_\ell}(\rho^2 - {\rho_\ell}^2) \end{cases}$$

III. Riemann problem

Given a pair of states (W_ℓ, W_r) the Riemann problem is the Cauchy problem associated with the system of conservation laws Eq. (4) and the initial condition

(10) $$W(x,0) = (W_\ell, W_r)\,,$$

and the solution is searched as self-similar $W(x,t) = V(\frac{x}{t}).$

It is supposed to be composed by four constant states $W_\ell, W_1^*, W_2^*, W_r$ separated by simple waves.

From the previous section (and details established in Ref. 13) the numerical resolution of the Riemann problem Eq. (4) and Eq. (10) consists essentially in finding the common pressure $p*$ and the common velocity $u*$ of the two intermediate states W_1^* and W_2^*. On the one hand, the state W_1^* belongs to the 1-wave issued from W_ℓ:

(11) $$u* = \begin{cases} u_\ell - c_\ell \log(\frac{p*}{p_\ell}), & p* \le p_\ell \\ u_\ell - c_\ell\left(\sqrt{\frac{p*}{p_\ell}} - \sqrt{\frac{p_\ell}{p*}}\right), & p* \ge p_\ell \end{cases}$$

on the other hand, the W_2^* belongs to the 4-wave arriving to W_r:

(12) $$u* = \begin{cases} u_r + c_r \log(\frac{p*}{p_r}), & p* \le p_r \\ u_r + c_r\left(\sqrt{\frac{p*}{p_r}} - \sqrt{\frac{p_r}{p*}}\right), & p* \ge p_r \end{cases}$$

The system of Eq. (11) and Eq. (12) is then solved with a standard Newton algorithm.

After the intermediate $u*$ velocity and pressure $p*$ are determined, the structure of the solution of the Riemann problem Eq. (4) and Eq. (10) is elementary to derive[13].

Godunov scheme

One introduces the solution $V(\xi, W_\ell, W_r)$ of the Riemann problem with initial condition (10) as a function of the similitude velocity $\xi \equiv \frac{x}{t}$. It is classical (see *e. g.* Ref. 12 or Ref. 14) that the flux function $\Phi_{\ell r}^G$ initially proposed by Godunov[15] is given by the relation

(13) $$\Phi_{\ell r}^G = f(V(0, W_\ell, W_r))$$

The numerical results of a first order scheme satisfying the following discrete volume framework

(14) $$\frac{W_j^{n+1} - W_j^{n1}}{\Delta t} + \frac{f(V(0, W_j, W_{j+1})) - f(V(0, W_{j-1}, W_j))}{\Delta x} = 0$$

are presented on Fig. 1

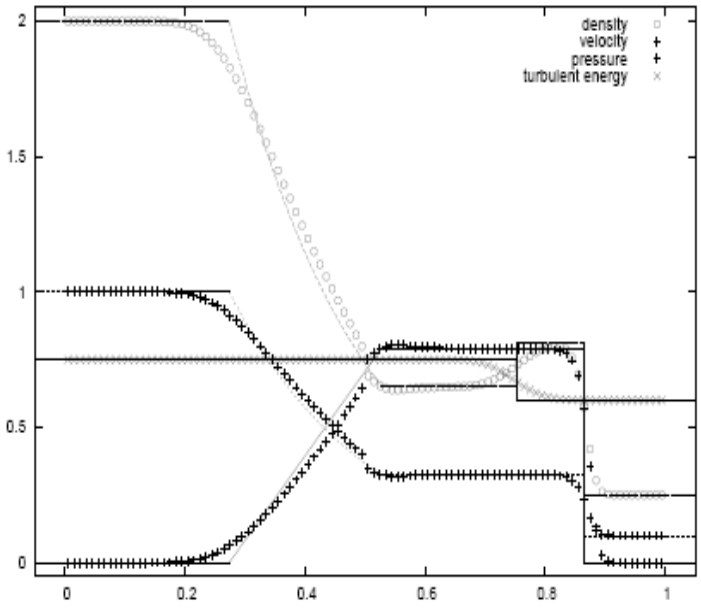

Figure 1. Approximate solution of particle-gas system with the Godunov scheme

Roe scheme

We have introduced in Ref. 11 a Roe matrix associated with the system defined by the constitutive relations Eq. (1) to Eq. (5). First, after the pioneering work of P. Roe[16], we introduce the total enthalpy H according to

(15) $$H = E + \frac{p}{\rho}$$

and consider the following mean values:

(16) $$\begin{cases} u^* = \dfrac{\sqrt{\rho_\ell}u_\ell + \sqrt{\rho_r}u_r}{\sqrt{\rho_\ell} + \sqrt{\rho_r}} \\ H^* = \dfrac{\sqrt{\rho_\ell}H_\ell + \sqrt{\rho_r}H_r}{\sqrt{\rho_\ell} + \sqrt{\rho_r}} \\ k^* = \dfrac{\sqrt{\rho_\ell}k_\ell + \sqrt{\rho_r}k_r}{\sqrt{\rho_\ell} + \sqrt{\rho_r}} \end{cases}$$

Then a so-called "Roe state" W^* is entirely defined and the associated sound velocity is simply given according to $c^* = \sqrt{(\gamma-1)k^*}$. The jacobian matrix $df(W^*)$ is given by the relation

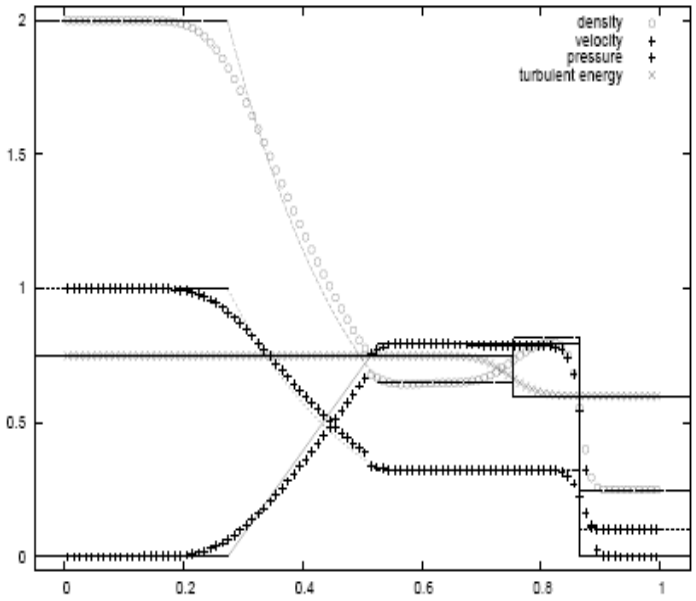

Figure 2. Approximate solution of particle-gas system with the Roe scheme

(17) $$df(W^*) = \begin{pmatrix} 0 & 1 & 0 & 0 \\ -(u^*)^2 & 2u^* & 0 & \gamma-1 \\ \_u^*H^* & H^* & u^* & (\gamma-1)u^* \\ -u^*k^* & k^* & 0 & u^* \end{pmatrix}$$

and it satisfies the fundamental relation introduced in Ref. 16:

(18) $$f(W_r) - f(W_\ell) = df(W^*) \bullet (W_r - W_\ell)$$

and is proven in Ref. 11.

After evaluation of the previous matrix, the associated eigenvectors r_j^* such that

(19) $$\begin{cases} df(W^*) \bullet r_1^* = (u^* - c^*) r_1^* \\ df(W^*) \bullet r_2^* = u^* r_2^* \\ df(W^*) \bullet r_3^* = u^* r_3^* \\ df(W^*) \bullet r_4^* = (u^* + c^*) r_4^* \end{cases}$$

are easy to specify. We have in particular

(20) $$r_1^* = \begin{pmatrix} 1 \\ u^* - c^* \\ H^* - (\gamma-1)k^* - u^*c^* \\ k^* \end{pmatrix} \quad r_4^* = \begin{pmatrix} 1 \\ u^* + c^* \\ H^* - (\gamma-1)k^* + u^*c^* \\ k^* \end{pmatrix}.$$

Then we can decompose the discontinuity $W_r - W_\ell$ along these waves,

(21) $$W_r - W_\ell = \sum_{j=1}^{j=4} \alpha_j r_j^*$$

and we obtain:

$$(22)\qquad \left[\begin{array}{l} \alpha_1 = \dfrac{\rho_r(c^* k_r - (u_r - u^*)k^*) + \rho_\ell((u_\ell - u^*)k^* - c^* k_\ell)}{2k^* c^*} \\ \alpha_4 = \dfrac{\rho_r((u_r - u^*)k^* + c^* k_r) - \rho_\ell((u_\ell - u^*)k^* + c^* k_\ell)}{2k^* c^*} \end{array}\right.$$

The Roe-flux $\Phi^R_{\ell r}$ is then easy to determine. The idea is to solve the Riemann problem between the two states W_ℓ and W_r with the flux f replaced by the following affine function:

$$(23)\qquad \Phi_{\ell r}(W) = f(W_\ell) + df(W^*) \bullet (W - W_\ell) \quad \equiv f(W_r) + df(W^*) \bullet (W - W_r)$$

We have after some lines of algebra (see Ref. 12 or Ref. 14):

$$(24)\qquad \Phi^R_{\ell r} = \left[\begin{array}{ll} f(W_\ell) & if \quad u^* - c^* > 0 \\ f(W_\ell) + \alpha_1(u^* - c^*)r_1^* & if \quad u^* - c^* \le 0 < u^* \\ f(W_r) - \alpha_4(u^* + c^*)r_4^* & if \quad u^* \le 0 < u^* + c^* \\ f(W_r) & if \quad u^* + c^* \le 0 \end{array}\right.$$

The results of the discrete integration are presented on Fig. 2.

Sanders and Prendergast splitting scheme

Using splitting scheme is very popular in computational fluid dynamics. In Ref. 10, the popular splitting scheme initially proposed by Sanders and Prendergast[17] for the perfect gas has been generalized for gas-particle modelling. The physical flux function f introduced in Eq. (3) is split into two parts:

$$(25)\qquad f(W) = f^+(W) + f^-(W)$$

With the following classical conditions, parameterized by the Mach number $M \equiv \dfrac{u}{c}$ and taking into account the particular value of Eq. (7) of the particulate sound velocity, we obtain for $|M| > 1$:

$$(26)\qquad \left[\begin{array}{l} f^+(W) = 0 \quad , \quad f^-(W) = f(W) \quad if \quad M \le -1 \\ f^-(W) = 0 \quad , \quad f^+(W) = f(W) \quad if \quad M \ge 1 \end{array}\right.$$

For the "subsonic" cases, following the approach of Ref. 17 where the particulate velocity is modelized by a 3 points discrete distribution {*u-c* , *u* , *u+c*}, we obtain

When $-1 \le M \le 0$,

$$(27)\qquad \left[\begin{array}{l} f^+(W) = \left[\begin{array}{c} f_m^+ \equiv \dfrac{p}{2c}(1+M) \\ f_m^+(u+c) \\ f_m^+(\iota + k - \dfrac{p}{2\rho}) + \dfrac{pc}{4}(M+1)^3 \\ f_m^+ k \end{array}\right] \\ f^-(W) = \left[\begin{array}{c} f_m^- \equiv \rho u - \dfrac{p}{2c}(1+M) \\ \rho u^2 + \dfrac{p}{2}(1 - 2M - M^2) \\ f_m^-(\iota + k - \dfrac{p}{2\rho}) + \dfrac{pc}{4}(M-1)^3 \\ f_m^- k \end{array}\right] \end{array}\right.$$

When $0 \le M \le 1$,

(28)

$$f^+(W) = \begin{bmatrix} f_m^+ \equiv \rho u + \frac{p}{2c}(1-M) \\ \rho u^2 + \frac{p}{2}(1+2M-M^2) \\ f_m^+(\iota + k - \frac{p}{2\rho}) + \frac{pc}{4}(M+1)^3 \\ f_m^+ k \end{bmatrix} .$$

$$f^-(W) = \begin{bmatrix} f_m^- \equiv \frac{p}{2c}(M-1) \\ f_m^-(u-c) \\ f_m^-(\iota + k - \frac{p}{2\rho}) + \frac{pc}{4}(M-1)^3 \\ f_m^- k \end{bmatrix}$$

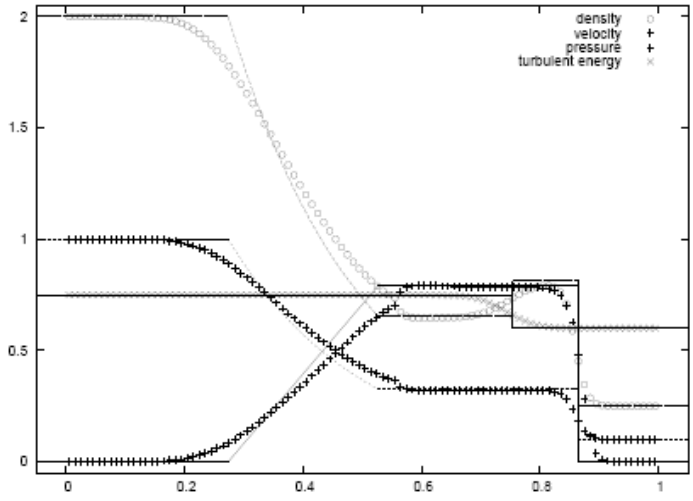

Figure 3. Approximate solution of the Sanders-Prendergast splitting scheme.

Then the numerical splitting scheme $\Phi_{\ell r}^{SP}$ is defined according to

(29) $$\Phi_{\ell r}^{SP} = f^+(W_\ell) + f^-(W_r).$$

The results of the discrete simulation are presented in Fig. 3:

Comparison of the 1D results :

We note that the two flux difference decomposition of Godunov and Roe are very similar, whereas the Sanders & Prendergast flux splitting exhibits more numerical viscosity. Nevertheless the three test cases indicate that the formulation is robust and validated for basic non viscous flow. This allows more complex developments and applications.

IV. Complete formulation in the PNS code

We describe here the specific features of the particulate pressure model, implemented in an axi-symmetric, two-phase, reactive and turbulent PNS code[18]:

Stress tensor and pseudo particle viscosity:

Let us start with the kinetic stress tensor for particle flow, described in Ref. 8, and proposed by Simonin[19]. It is expressed here in classical tensor notation and contraction:

(30) $$\langle u'_{p,i}\, u'_{p,j} \rangle = -\nu_p(\frac{\partial U_{p,i}}{\partial x_j} + \frac{\partial U_{p,j}}{\partial x_i}) + (\gamma - 1)\delta_{ij}(k_p + \nu_p \frac{\partial U_{p,l}}{\partial x_l}),$$

where $U_{p,i}, u'_{p,i}$ are the Cartesian components of mean and fluctuating particle velocity. By definition, the trace of the tensor must be $2k_p$, and k_p is the fluctuating kinetic energy, identical to k in the previous section, but the subscript p is now needed to distinguish with the gas variables. This leads to the value of the parameter γ:

(31) $$\gamma = \frac{5}{3}$$

The energy k_p is defined by

(32) $$k_p = \frac{1}{2}(u_p'^2 + v_p'^2 + w_p'^2).$$

By setting then Eq. (5):

(33) $$P_p = \frac{2}{3}\rho_p k_p,$$

we recognize some similarities with the Reynolds stress tensor as described by Wilcox[20] and the Boussinesq approximation. Following Simonin[19], the particle pseudo-viscosity is:

(34) $$\nu_p = \frac{1}{3}k_{fp}T^* + \frac{2}{3}k_p\langle\tau_p\rangle.$$

The first right-hand term is the direct relation with the turbulent gas (it is 0 in laminar gas flow). k_{fp} is the trace of the covariance matrix, where subscript f refers to the gas (fluid):

(35) $$k_{fp} = \langle u'_{f,i}\, u'_{p,j}\rangle.$$

T^* is related to the Taylor integral time scale , and can depend on particle inertia: We retain from Ref. 8

(36) $$T^* = 0.2\frac{k_f}{\varepsilon_f}cor.$$

k_f is the gas turbulent kinetic energy and ε_f the associated dissipation. $cor < 1$ is a correction term to take account of crossing trajectory effect[8].

The 2nd right hand term in Eq. (34) is related to the mean particle relaxation time, which is a fundamental parameter.

(37) $$\langle\tau_p\rangle = \frac{4d(\rho_{p,material} + 0.5\rho_f)}{3\rho_f\langle C_D\rangle\langle|U_R|\rangle},$$

Where d is the particle diameter, $\langle C_D\rangle$ the mean particle drag coefficient, $\langle U_R\rangle$ the mean relative velocity $U_R = \left|\vec{V}_p - \vec{V}_f\right|$, and $\rho_{p,material}$ is the material density of the particle**.** The variable τ_p characterizes the time response of the particle to fluid solicitation, it depends on inertia and drag force.

Governing equation:

At this step, we can reconstruct the governing equation as for the NS equation of gas with an additional k equation. Note that the pressure term in Eq. (33) is extracted from the tensor of Eq. (30) multiplied by ρ_p, to form the conservative variables for momentum and total energy, whereas for the k_p equation, Eq. (33) is maintained in the production term.

The following system is obtained for particles. It contains 5 conservation equations: one for mass, 2 for momentum (2D cylindrical), one for total energy, and one for fluctuating kinetic energy k_p:

$$\frac{\partial(r(\overline{E} - \overline{Ev}))}{\partial\xi} + \frac{\partial(r(\overline{F} - \overline{Fv}))}{\partial\eta} + \overline{S''} = 0$$

(38) $$\overline{E} = \frac{\xi_x}{J}E + \frac{\xi_y}{J}F \qquad \overline{F} = \frac{\eta_x}{J}E + \frac{\eta_y}{J}F$$

$$E = (\rho_p u_p, \rho_p u_p^2 + P_p, \rho_p u_p v_p, \rho_p H_p u_p, \rho_p k_p u_p)$$

$$F = (\rho_p v_p, \rho_p u_p v_p, \rho_p v_p^2 + P_p, \rho_p H_p v_p, \rho_p k_p v_p),$$

The expression of total enthalpy H_p, consistent with Eq. (1) and Eq. (3) is:

(39) $$H_p = C_p T_p + \frac{1}{2}(u_p^2 + v_p^2) + k_p + \frac{P_p}{\rho_p} = C_p T_p + \frac{1}{2}(u_p^2 + v_p^2) + \frac{5}{3}k_p,$$

The system of Eq. (38) is written in a conservative form (multiplication by radial coordinate r, inside the derivatives).A classical transformation is used (x,r) ➔ (ξ,η) where $\xi = x$ is the axial direction and η is a non dimensional function of r and rmax(x), with a stretching function to refine mesh around a specified radial position.

The Eulerian fluxes $\overline{F}$ are computed in cylindrical coordinates for the Roe scheme or the flux splitting scheme, following the state of the art described in section III.

$\overline{Ev}$ and $\overline{Fv}$ are the pseudo viscous fluxes, also originating from the tensor of Eq. (30) for momentum. Note that we apply the PNS approximation by setting $\overline{Ev} = 0$ and by implementing a space-marching process in the x direction (Fig. 4). The gas and particle meshes are the same.

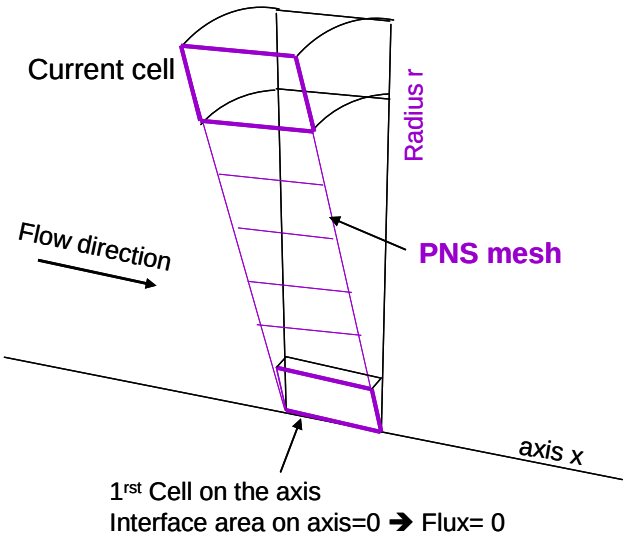

Figure 4. PNS mesh.

System closure:

The inter-particular collisions are neglected, so the associated dissipation term in the k_p equation is 0.

Moreover, the third order correlation tensor is set to 0.

We choose not to add a supplementary equation for the covariance k_{fp}, but to propose a closure based on Tchen theory[21]:

$$k_{fp} = \frac{2k_f}{1+St^*}, \tag{40}$$

Where St^* is the Stokes number:

$$St^* = \frac{\langle \tau_p \rangle}{T^*}. \tag{41}$$

Source terms:

The $\overline{S''}$ term in Eq. (38) involves different source terms that will be detailed. The first one is the production term in the k_p equation: The same formalism as for gas turbulence (see for instance Ref. 20) is used (production term on left hand side, tensor notation: this is a contraction of 2 tensors, giving a real):

$$P_{kp} = \rho_p \langle u'_{p,i} u'_{p,j} \rangle \otimes \frac{\partial U_{p,i}}{\partial x_j}, \tag{42}$$

P_{kp} is expressed in 2D cylindrical coordinates in the PNS code. The expression, replaced right hand side in Eq. (38), becomes:

$$-P_{kp} = -P_p div\vec{V}_p - \frac{2}{3}\rho_p \nu_p (div\vec{V}_p)^2 + \rho_p \nu_p \left((rotVp)^2 + (gradVp)^2 \right), \tag{43}$$

where the first right hand side term plays an important role for convergent particle flows. The velocity divergence $div\vec{V}_p$ is then negative, and the production term of k_p is increased, so that pressure and pseudo viscosity are increased, acting as accumulation solvers.

Following Oesterlé[8] and Simonin[19] the source term (on left hand side) in the k_p equation is:

(44) $$M'_{kp} = \frac{\rho_p}{\langle \tau_p \rangle}(2k_p - k_{fp}),$$

In the total particle energy equation, it is correct to repeat the term in Eq. (44) and to add the more classical term of the work of the drag force (source term on left hand side):

(45) $$M'_{drag\_work} = \frac{\rho_p}{\langle \tau_p \rangle}\vec{U}_p.\vec{U}_R$$

Also two classical source terms, the heat exchanges between gas and particles and the particle radiation are not detailed here.

The important coupling in momentum equations is (for the velocity components i=1,2; and source term on left hand side)**:**

(46) $$M'_{p,i} = \frac{\rho_p}{\langle \tau_p \rangle}U_{R,i},$$

Where $U_{R,i}$ is defined as:

(47) $$U_{R,i} = U_{p,i} - U_{f,i} - U_{D,i},$$

The expression introduces the drift velocity $U_{D,i}$, explained by Oesterlé[8] and proposed by Simonin[22] $U_{D,i}$ is related to the turbulent diffusion of particles, which can be caused by particulate density gradient, non-homogeneous turbulence, or physical accumulation due to vortex. We also add the formulation for drift velocity of Bocksell and Loth[23], based on the gradient of the gas turbulent kinetic energy, and the eddy and particle lifetimes (see section V).

Note also two classical additional source terms in the radial velocity equation, due to conservative formulation and Reynolds stress $\sigma_{\theta\theta}$ in the orthogonal direction, not detailed here.

Coupling with the gas:

The gas PNS system with a turbulent (k_f, ε_f) model, is a 6-equations system (one for mass, 2 for momentum (2D cylindrical), one for total energy, one for fluctuating kinetic energy k_f and one for the dissipation ε_f. In the gas momentum and the gas total energy equations, the coupling terms are exactly the opposite. For example we have for one particle size type:

(48) $$M'_{f,i} = -M'_{p,i}$$

The PNS code can deal with several particle types (characterized by different sizes). They act independently and coupling is only performed through the gas. The gas source term in Eq. (48) is then the sum of the particle contributors.

Following Ref. 8, the coupling with the k_f equation for gas is not straightforward: firstly it introduces the drift velocity, secondly it distinguishes the turbulence generated by the wake of each particle, from the turbulence at large scale. The added expression is: (source term on left hand side in the gas turbulent energy k_f equation)

(49) $$M'_{kf} = -\frac{\rho_p}{\langle \tau_p \rangle}(k_{fp} - 2k_f + \vec{U}_D.\vec{U}_R)$$

Again, following Ref. 8 the added source term in the gas turbulent dissipation equation ε_f is**:**

(50) $$M'_{\varepsilon f} \approx 1.8\frac{\varepsilon_f}{k_f}M'_{kf}.$$

V. First applications

Firstly an important verification is performed: for a solid rocket plume calculation, imposed in laminar gas regime: The two options of the present particulate pressure model (Flux splitting and Roe schemes) are run with the

particulate pressure imposed at a very low value, so that the detailed formulation is computed at the limit of the model. The results are compared with the initial PNS without particulate pressure ("donor cell" scheme). They were similar (in the computer precision range): this validates the correct coding of the new schemes.

Secondly, a high altitude solid rocket plume is computed, again with the two options of the particulate pressure model, and the initial PNS without particulate pressure. High altitude plume from an expanded nozzle exhibits no compression or convergent particle flow ($div\vec{V}_p$ is positive quite everywhere). It was satisfactory that the results indicate low differences with the case without particulate pressure.

Thirdly we evaluate the present method by comparison with published application cases, and we choose a particle dispersion case in a jet-like flow, proposed and tested by Papp, York, Sinha and Dash[24].

Finally we propose. a case of a compressed jet , where axial accumulation of particles can numerically occur.

Modelling consideration:

For these applications we consider first the classical model, where particles are solved as an eulerian gas without pressure. The system (38) is then reduced to:

$$\frac{\partial(r\overline{E})}{\partial\xi}+\frac{\partial(r\overline{F})}{\partial\eta}+\overline{S''}=0$$

(51) $$E=(\rho_p u_p,\rho_p u_p^2,\rho_p u_p v_p,\rho_p H_p u_p)\,.$$

$$F=(\rho_p v_p,\rho_p u_p v_p,\rho_p v_p^2,\rho_p H_p v_p),$$

There is no particle pressure, and no pseudo viscous term. The source terms (46), (47) contain no drift velocity, and there are no source terms (49) and (50). This model is called "w/o Pp (particulate pressure)". The numerical scheme is a classical "Donor Cell".

We compare this early formulation with the present one, called "with Pp" and described in section IV. In particular the expression of the drift velocity is:

(52) $$U_{D,i}=-\frac{1}{3}k_{fp}T^*\frac{1}{\rho_p}\frac{\partial\rho_p}{\partial x_i}+\frac{1}{3}\Delta t\frac{\partial k_f}{\partial x_i},$$

The first term on the right is related to the particulate density gradient Ref. 8. The second term, proposed by Bocksell and Loth[23] and also retained by Papp, York, Sinha and Dash[24], relates the drift to the gradient of gas turbulence and a characteristic time $\Delta t:\Delta t$ is the shortest time of the eddy life time, and the crossing time of the eddy by the particle. Theses terms are important in the radial direction.

To illustrate the effect of the drift velocity, we compare the applications of the present formulation and a formulation without drift, called "with Pp, w/o drift".

All applications are performed with two-way coupling and PNS space marching.

High speed shear layer , d=0.1µm:

The conditions of the shear layer case, proposed by Ref. 24, are given in table 1. It is the turbulent interaction of two streams. Stream 1 contains very small solid alumina particles at a low dilution rate (initial particle volume ratio=4.5E-06).

Variable	Stream 1	Stream 2
Mach	2.41	0.723
T(K)	1000	300
U(m/s)	1531.1	251.6
P(Pa)	101325	101325
ρp kg/m3)	0.018	-
Al2O3 d(µm)	0.1	-

Table 1: high speed shear layer

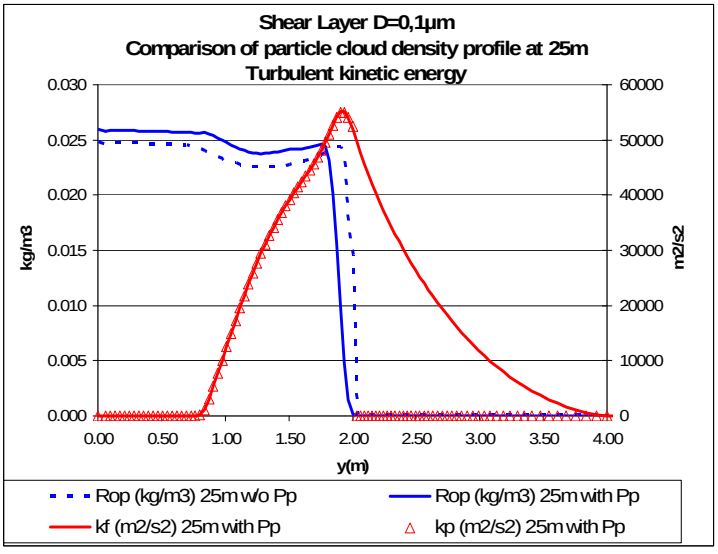

Figure 5.

According to a pressure split technique, the PNS approach is allowed in the subsonic stream. Here in 2D cylindrical coordinates, the entry section of stream 1 has a radius of 2m, so it compares well with the planar shear layer of Ref. 24.

Figure 5 represents particle cloud density profile at 25m from the initial section. We notice that for these small particles, there are little differences between the approaches, and that the particle dispersion is low. Comparison of gas and particle turbulent kinetic energy indicates that they are in phase, when both are present.

Comparisons of velocities in Fig. 6, indicate that the fluid and particles remain in phase.

For non stressing cases, it's important to notice here, that the results with the present formulation remain consistent with the early approach without particulate pressure.

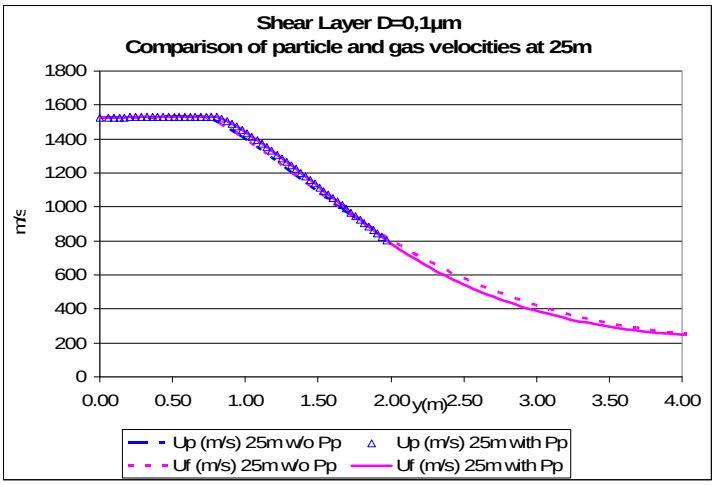

Figure 6.

High speed shear layer, d=10µm:

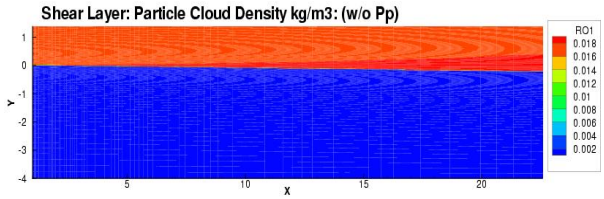

Figure 7

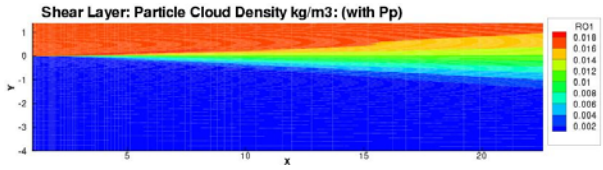

Figure 10

The conditions of the shear layer case of table 1 are the same, except for the 10µm particle diameter. Figure 7 shows the particle cloud density contours computed by the previous model without particle pressure. It is very similar to the results of Ref. 24 without dispersion.

The cloud density profiles in the region affected by gas turbulent kinetic energy exhibit an increase to the edge of the cloud, before abruptly vanishing (see Fig. 8). Furthermore, this abrupt edge is slightly extended outward when progressing in x stations:

Results are very different with the present formulation with particulate pressure: there is a more important dispersion of the particles, with no peak at the edge (Fig. 9 and Fig 10):

The shape of this new profile is similar to the shape of the lagrangian profile with drift velocity in Ref. 24.

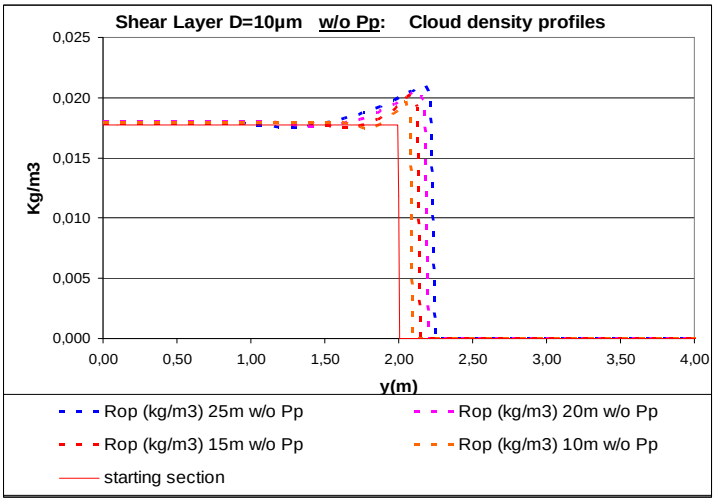

Figure 8.

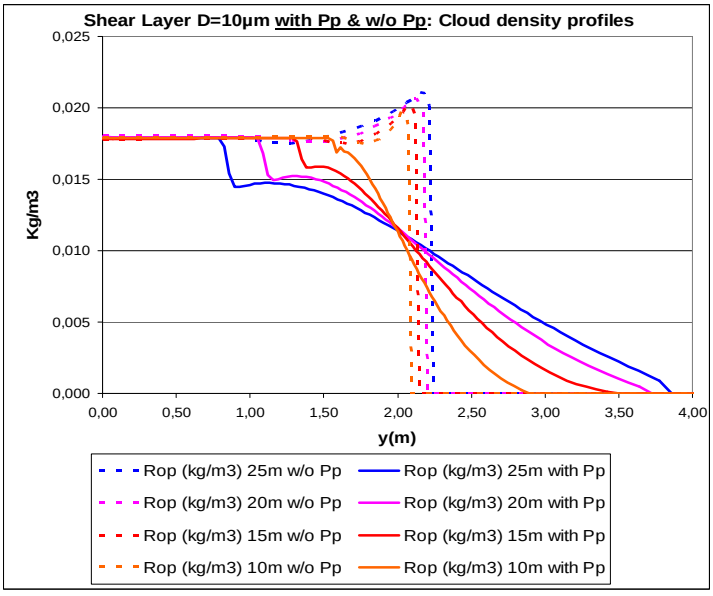

Figure 9.

The contours of the gas turbulent kinetic energy are similar for the early formulation (Fig. 11)and the present one (Fig. 12) and are very close in level and shape to the result in Ref. 24.

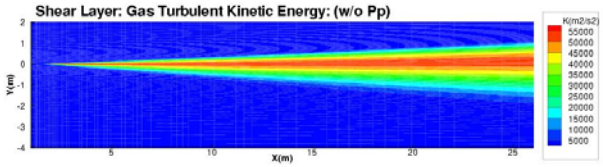

Figure 11

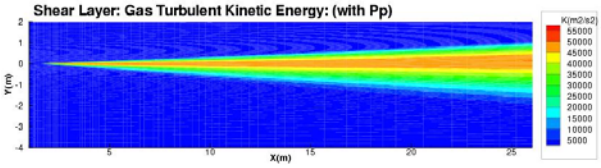

Figure 12

However, due to the damping effect of particles on turbulence, the levels in Fig. 12 are slightly lower. The gas velocity and the turbulent viscosity contours are represented in Fig. 13 and Fig. 14. Again they are comparable to

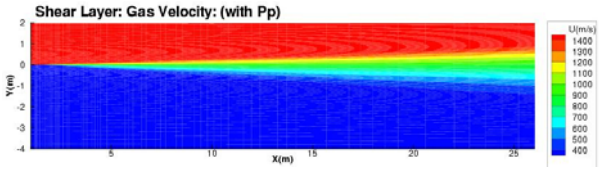

Figure 13

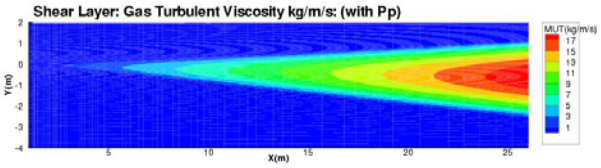

Figure 14

results in Ref. 24.

These new results are presented for the adapted Sanders & Prendergast numerical scheme. Results with the Roe scheme indicate a very small difference at the cloud boundary (Fig. 15). The ROE scheme has less numerical smearing. According to the very different approaches of the schemes, the comparison is satisfactory.

Figure 16 compares the particulate turbulent energy kp with the turbulent kinetic energy kf of the gas. Now there is a difference with Fig. 5 (D=0.1µm): the level of kp is lower than kf, as a consequence of particle size.

In Fig. 17, the velocities of gas and particles are presented together at different sections: the particles present almost no phase difference with the gas.

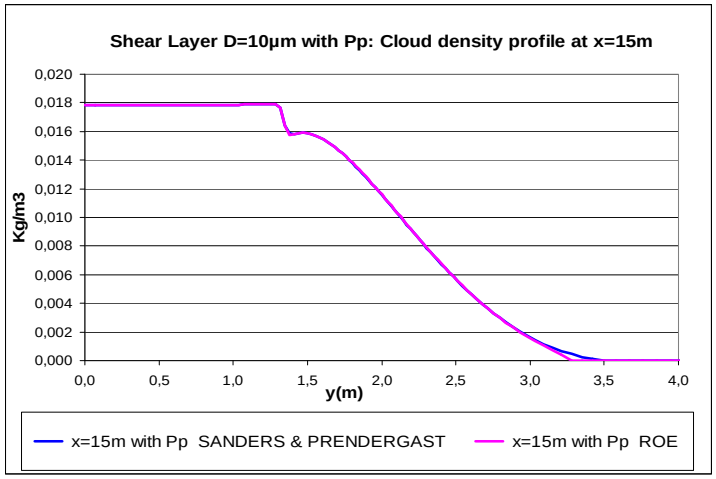

Figure 15.

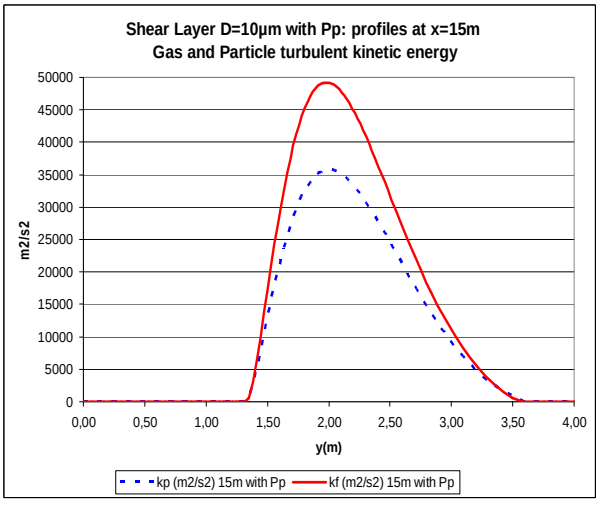

Figure 16.

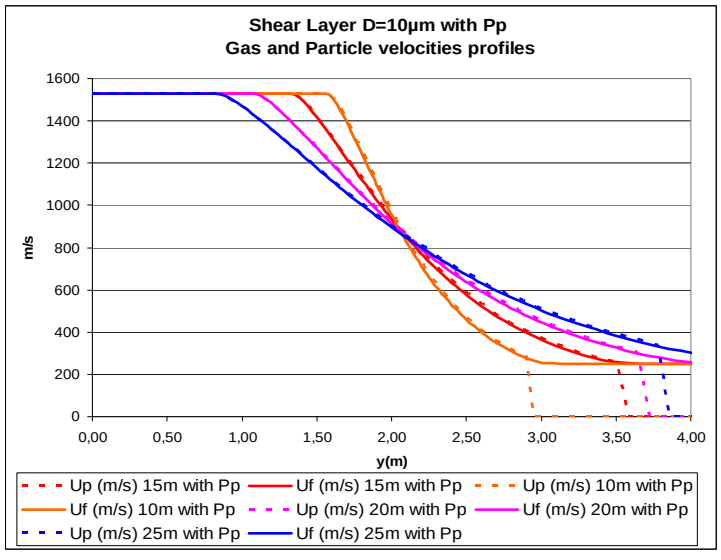

Figure 17.

High speed shear layer, d=10µm, w/o drift velocity:

Here we show results with no drift velocity in Eq. (47). Figure 18 exhibits important peaks in the particle cloud density profiles, located at the inner boundary of turbulence. The inflexion of Fig. 9 is removed, but at the expense of particle accumulation.

The accumulation is located at the sharp increase of turbulent kinetic energy (Fig. 19). And to correct this artefact, the drift velocity proposed by Bocksell and Loth[23] is needed. The formulation is efficient because it is based on the gradient of kf.

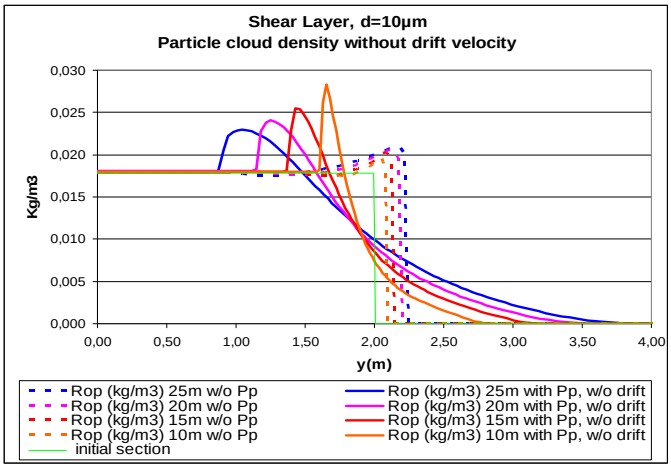

Figure 18.

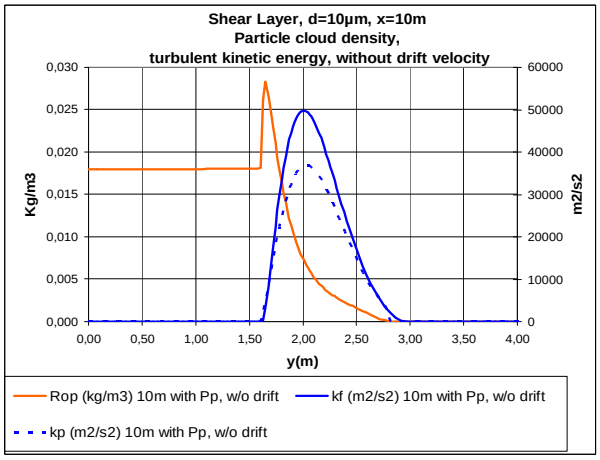

Figure 19.

Note that the same kind of peak, is reported in Ref. 24 for lagrangian calculation without drift velocity.

Compressed jet, d=10µm:

We propose this test case to describe axial accumulation and its resolution. The simulation does not represent any real or experimental case. We just increase the strength of stream 2. Stream 1 is a uniform round jet (1 meter radius) where 10µm particle are diluted (as in the previous case). The starting conditions are given in table 2:

Variable	Stream 1	Stream 2
Mach	1.5	2.5
T(K)	426	1000
U(m/s)	617	1576
P(Pa)	101325	101325
ρp (kg/m3)	0.039	-
Al2O3 d(µm)	10	-

Table 2: compressed jet

Figure 20 shows the particle cloud density contours, for the early formulation without particulate pressure.

Before 30m an axial accumulation occurs, and then increases to reach a dramatic factor 5 of the initial particle cloud density (and even more, downstream). The starting point is correlated with turbulence reaching the symmetry axis, as can be seen on Fig. 21.

With the present modelling with particulate pressure and drift velocity, the problem almost disappears (Fig. 22)

Also the gas turbulent kinetic energy is decreased in level (-10% compared to Fig. 21), in the region where

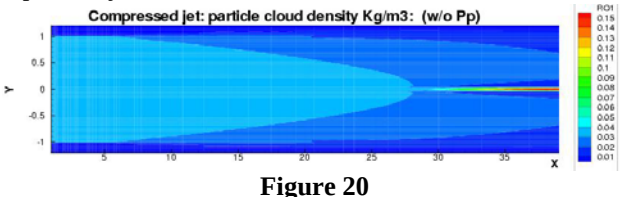

Figure 20

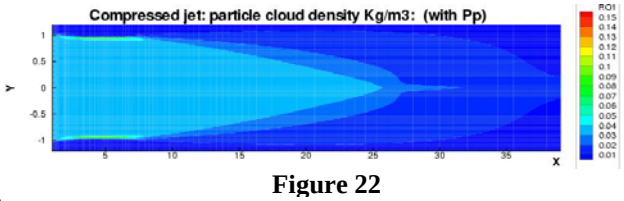

Figure 22

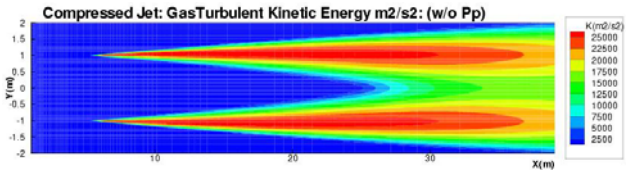

Figure 21

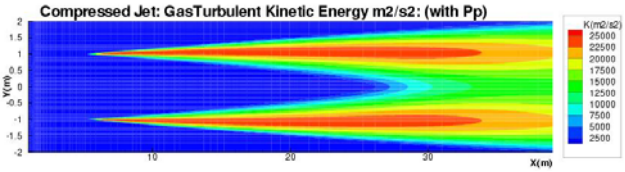

Figure 23

there are sufficient particles to act for turbulence damping (see Fig. 23 and Fig. 24).

Note in Fig. 25 the behaviour of the turbulent particulate kinetic energy, which drives the associated pressure Pp. Especially near the axis, it is closer to the gas turbulent kinetic energy. This, in conjunction with drift velocity, helps cancelling the numerical accumulation on the axis.

At the outer boundary of the cloud there is still some trouble with kp. The interface with the no-particle domain has always been difficult, and work remains to be done on that problem.

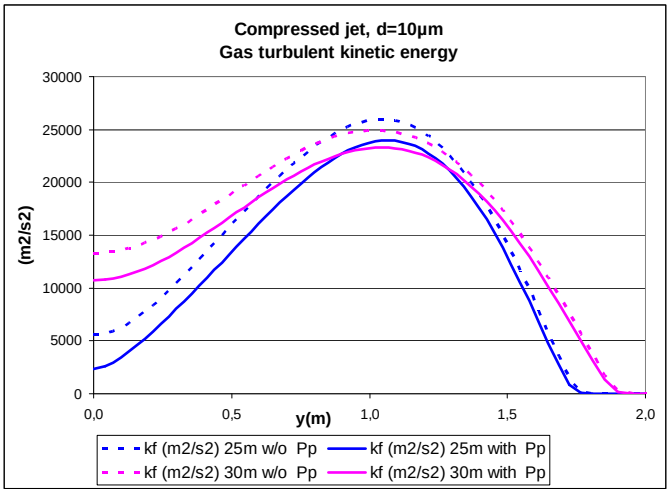

Figure 24.

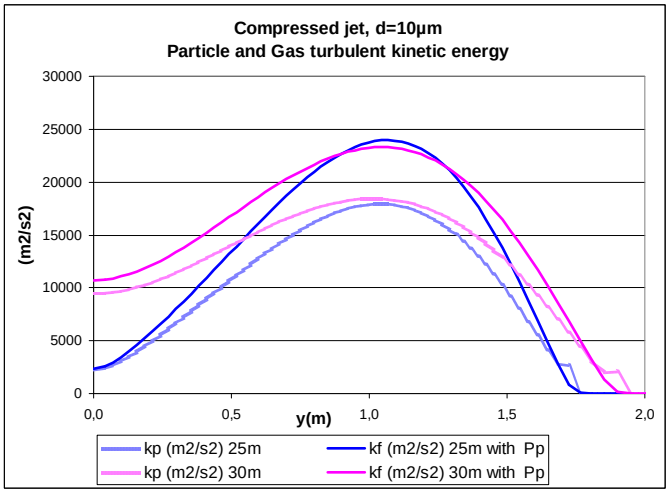

Figure 25.

The profiles of the particle cloud density are shown in Fig. 26 and Fig. 27: The present new formulation is efficient, especially at x=30m and x=35m in Fig. 27.

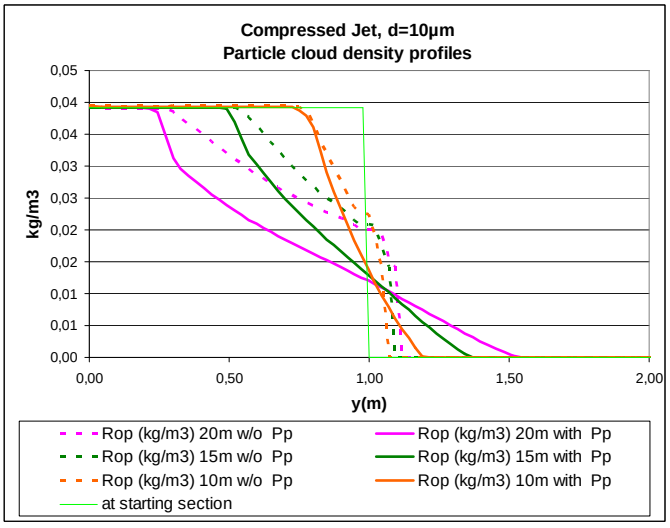

Figure 26.

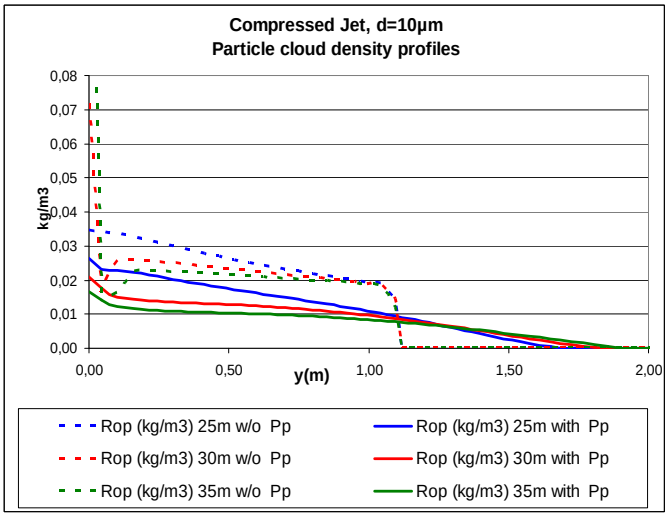

Figure 27.

Implementation of the present particulate pressure model in a fully 3D NS code[25] is under work.

VI. Conclusion

Engineers have to carefully analyze their CFD results for problems dealing with particles and their interaction with turbulence:

- The phenomenology is complex and contains multiple time scales.
- The classical Eulerian formulation without particulate pressure admits singular solutions for convergent flows (accumulations) that are not realistic for a dispersed phase. This characteristic has to be cured by an additive modelization.
- In some real cases, physical accumulation of particle occurs (near walls…).

This work shows some progress in the modeling and comparisons to others. The framework of the eulerian approach with particulate pressure and drift velocity, associated with a PNS space marching, allows rapid calculation with fine mesh, and solves unphysical accumulation problems in the free field. . It is believed that the unwanted accumulation is not related to the eulerian or the lagrangian solvers for particles. Also it is not related to the use of a specific numerical scheme for the Riemann problem, if it is well formulated.

Since source terms are related to gradients and then to the space discretization, it can occur that they explode near discontinuities (like the usual k-ε model). So, special care to maintain a realizable stress tensor may help. It is included in the present work but not detailed in this paper.

Additional study is necessary to explore remaining deficiencies and calibrate the model. Use of CFD for complex but real problems of gas/particle turbulent interaction is a challenge, which may be achievable.

So far, these kinds of density peaks of particle cloud are not reported in experimental data, but accumulation exist in the physics. This is also challenging for the validation. There is a real need of experimental reference tests, including two-phase flows with particles interacting with turbulence, at a relatively high speed.

Acknowledgments

This work was sponsored by EADS Astrium-ST. The authors would like to acknowledge Michel POLLET, Laurent CARITEY of EADS Astrium-ST for their efficient support, and accurate revue and comments. Also the authors acknowledge François CORON, manager of Thermal Mechanical Engineering directorate, for encouraging this team work.

References

[1]J. Ferry, S. Balachandar, F. Najjar. AIAA 2000-3569. *Fundamental Two phase Modeling Efforts at CSAR*

[2]R. Saurel, E. Daniel, J.C. Loraud. *Treatment of symmetry boundary condition for two phase dilute flows*. Two phase flow modelling and experimentation. 1995 Edizioni ETS

[3]R. Saurel, R. Abgrall. *A multiphase Godunov method for compressible multifluid and multiphase flows*. J. Comput. Phys, Vol. 150, p.425-467, 1999.

[4]O. Simonin. *Theoretical and experimental modelling of particulate flow, part I: Theoretical derivation of dispersed phase Eulerian modelling from probability density function kinetic equation*. Lecture Series Programme 200-06, Von Karman Institute, 2000

[5]M. Simoes. *Modélisation eulérienne de la phase dispersée dans les moteurs à propergol solide, avec prise en compte de la pression particulaire*. PhD Thesis, INP Toulouse, 2006.

[6]M. Simoes, P. Della Pieta, F. Godfroy, O. Simonin. *Continuum Modeling of the Dispersed Phase in Solid Rocket Motors.* AIAA 2005-4698

[7]M. Simoes, O. Simonin. *Modeling of particulate pressure in the frame of mesoscopic Eulerian formalism for compressive reactive two phase flows***.,** 2006 Joint US European Fluids Engineering Summer Meeting July 17-20 MIAMI

[8]B. Oesterlé. *Ecoulements multiphasiques : des fondements aux méthodes d'ingénierie.* Hermes Science Lavoisier 2006

[9]L.D. Landau, E.M. Lifchitz. *Fluid Mechanics*. Pergamon Press, London, 1959.

[10]C. Hug. *Formulation Navier Stokes Parabolisé à pression particulaire pour des écoulements diphasiques laminaires et turbulents en 2D axisymétrique (PNS code V16)*. Astrium ST, Internal report, October 2008.

[11]F. Dubois. *Un système hyperbolique pour un gaz de particules*. Manuscript, 27 October 2008.

[12]E. Godlewski, P.A. Raviart. *Numerical approximation of hyperbolic systems of conservation laws*. Springer, New York, 509 p, 1996.

[13]F. Dubois. *Problème de Riemann pour le système de gaz de particules*, Manuscript, 20~April 2009.

[14]B. Després, F. Dubois. *Systèmes hyperboliques de lois de conservation : Application à la dynamique des gaz*, Editions de l'Ecole Polytechnique, 201 p., 2005.

[15]S.K. Godunov. *A Difference Scheme for Numerical Solution of Discontinuous Solution of Hydrodynamic Equations*. Math. Sbornik, 47, p.~271-306, 1959. Translated US Joint Publ. Res. Service, JPRS 7226, 1969.

[16]P. Roe. *Approximate Riemann solvers, parameter vectors and difference schemes*. J. Comput. Phys., 43, p.357-372, 1981.

[17]R. Sanders. K. Prendergast. *The possible relation of the three-kiloparsec arm to explosions in the galactic nucleus.* Astrophys. J.,188, p. 489-500, 1974.

[18]C. Hug, L. Fusade, M. Pollet, P. Brenner, JC. Astier, *Jets de propulseurs et leurs signatures.* 36ème Colloque d'Aérodynamique Appliquée AAAF, Orléans, 20-22 mars, 2000

[19]O. Simonin. *Modélisation au second ordre du mouvement fluctuant des particules dans les écoulements diphasiques turbulents.* Rapport 93NB00010, EDF, 1993

[20]D. C. Wilcox. *Turbulence Modeling for CFD*. 2nd edition 2004

[21]C. M. Tchen. *Mean value and correlation problems connected with the motion of small particles suspended in turbulent fluid.* PhD Thesis 1947

[22]O. Simonin, Viollet P.-L. *Modelling of turbulent two-phase jets loaded with discrete particle*. Eds Phase-Interface Phenomena in Multiphase Flows, Hemisphere Publ. Corp., New York, p.259,269, 1990

[23]T. L. Bocksell and E. Loth. *Random Walk Models for Particles Diffusion in Free-Shear Flows.* AIAA vol. 39., N° 6, June 2001

[24]J.L. Papp, B.J. York, N. Sinha and S.M. Dash. *Progress in Modeling Particle Jets/Plumes.* AIAA 2003-1284

[25]M. Pollet, P. Brenner. *Aerodynamics with Moving Bodies Applied to Solid Propulsion.* AIAA paper 89-2779,1989